Published in final edited form as:
Am J Physiol Heart Circ Physiol. 2007 March ; 292(3): H1568–H1578.

Spatial Heterogeneity of the Restitution Portrait in Rabbit Epicardium

Ann M. Pitruzzello[1], **Wanda Krassowska**[1,2], and **Salim F. Idriss**[1,3]

1*Department of Biomedical Engineering, Medical Center, Durham, North Carolina, USA*

2*Center for Nonlinear and Complex Systems, Duke University, Medical Center, Durham, North Carolina, USA*

3*Department of Pediatrics, Division of Pediatric Cardiology, Duke University, Medical Center, Durham, North Carolina, USA*

Abstract

Spatial heterogeneity of repolarization can provide a substrate for reentry to occur in myocardium. This heterogeneity may result from spatial differences in APD restitution. The restitution portrait (RP) measures many aspects of rate-dependent restitution: the dynamic restitution curve (RC), S1-S2 RC, and short-term memory response. We used the RP to characterize epicardial patterns of spatial heterogeneity of restitution that were repeatable across animals. NZW rabbit ventricles were paced from either the epicardial apex, mid-ventricle, or base, and optical action potentials were recorded from the same three regions. A perturbed downsweep pacing protocol was applied that measured the RP over a range of cycle lengths from 1000-140 ms. The time constant of short-term memory measured close to the stimulus was dependent on location. In the mid-ventricle the mean time constant was 19.1±1.1 sec, but it was 39% longer at the apex ($p<0.01$) and 23% longer at the base ($p=0.03$). The S1-S2 RC slope was dependent on pacing site ($p=0.015$), with steeper slope when pacing from the apex than from the base. There were no significant repeatable spatial patterns in steady-state APD at all cycle lengths or in dynamic RC slope. These results indicate that transient patterns of epicardial heterogeneity of APD may occur following a change in pacing rate. Thus, it may affect cardiac electrical stability at the onset of a tachycardia or during a series of ectopic beats. Differences in restitution with respect to pacing site suggest that vulnerability may be affected by the location of reentry or ectopic foci.

Keywords

rate dependence; short-term memory; dynamic restitution curve; S1-S2 restitution curve; action potential duration

Introduction

Cardiac tissue heterogeneities are thought to increase vulnerability to arrhythmias. These heterogeneities take the form of anatomical obstacles (44), such as coronary vessels, papillary muscles, or infarcted regions, or they arise from physiologic causes such as tissue anisotropy (47), regional differences in ion channel densities (2), and intrinsic spatial variations in action potential duration (APD) that exist transmurally (2,16) or in different parts of the heart (23, 29). The latter, spatial heterogeneity of APD, has received considerable attention in recent years because APD differences can cause dispersion of repolarization, creating a situation in

Address for correspondence: Ann M. Pitruzzello, Duke University, Department of Biomedical Engineering, Box 90281, Durham, NC 27708, 919-660-5113, 919-684-4488 (fax), ann.pitruzzello@duke.edu

which a premature stimulus can cause unidirectional block and thus initiate reentry (1). In the diseased heart, these APD differences can be greatly enhanced, leading to marked heterogeneity of repolarization that can cause conduction block in the absence of premature stimulation (3,33).

Often, the existence and the magnitude of spatial APD differences depend on the pacing rate. Thus, electrical restitution, i.e., the relationship between APD and the preceding diastolic interval (DI) is the fundamental tool in investigating the stability of cardiac rhythm. Specifically, steepness of the APD restitution curve (RC) has been linked to arrhythmogenesis, with steeper curves associated with alternans, a pattern of alternating long and short APDs occurring at fast pacing rates (27). Even in a homogeneous tissue, different regions can alternate out of phase (discordant alternans), causing dispersion of repolarization, unidirectional block, and eventually reentry (10,30,34). Similarly, a single premature stimulus can cause dispersion of repolarization and initiate reentry (1,21). Thus, the onset of an arrhythmia can be precipitated by “functional” APD heterogeneities that occur due to purely dynamical processes. Intrinsic tissue heterogeneities can work synergistically with functional heterogeneities, greatly increasing vulnerability to arrhythmia (44). However, little is currently known about spatial heterogeneity of both transient and steady-state restitution.

To date, restitution has typically been characterized by the dynamic RC (which measures steady-state APD at fixed basic cycle lengths [BCLs]) or by the S1-S2 RC (which measures APD following premature or postmature stimuli when pacing at a fixed BCL). The restitution portrait (RP) was developed as a tool for measuring and visualizing multiple aspects of APD restitution simultaneously (20). In addition to the dynamic RC and S1-S2 RC, the RP includes a transient response that arises from short-term cardiac memory. The short-term memory response (also called APD accommodation) is the slow monotonic change in APD following a sustained change in pacing rate. This response is a measure of the amount of memory present with respect to pacing history and occurs on a time scale of minutes (11,20,36,45). It should be noted that this response is distinct from long-term memory changes that involve electrical remodeling and occur on time scales of hours or longer (37). The dynamic, S1-S2, and short-term memory responses, measured for a series of BCLs and visualized simultaneously in a RP, give a comprehensive assessment of both transient and steady-state aspects of restitution.

Our study is the first measurement of the RP in the perfused mammalian ventricle in vitro; previously, the RP has been measured in superfused frog ventricular tissue (20) and isolated rabbit and guinea pig myocytes (40). Likewise, this is a first study that investigates spatial differences in the restitution portrait; previous studies involved either single cells (40) or were limited to only one or two microelectrode impalements (20). We differentiate in this study between heterogeneity of restitution that forms spatial patterns repeatable from animal to animal and heterogeneity with no consistent spatial patterns. The former is generally attributed to varying ion channel densities in different regions of tissue. The cause of the latter is not known, but many have studied such dispersion of restitution because the degree of dispersion is thought to affect rhythm stability (21,25). This study focuses on the former: we use the RP to characterize repeatable gradients of restitution properties from apex to base in rabbit epicardium.

Methods

Isolated Left Ventricle Preparation

Experiments were performed on 14 adult New Zealand White rabbits (3.8 ± 0.5 kg), 6 female and 8 male, following a protocol approved by the Duke University Institutional Animal Care and Use Committee. Rabbits were premedicated with intramuscular ketamine (35 mg/kg) and xylazine (5 mg/kg), then given intravenous heparin (800 U/kg) followed by thiopental sodium

(20 mg/kg). Hearts were rapidly excised and submerged in cold, oxygenated high-potassium Tyrode′s solution containing 123 mM NaCl, 11 mM dextrose, 20 mM $NaHCO_3$, 24 mM KCl, 1.0 mM $NaH_2PO_4 \cdot H_2O$, 1.1 mM $MgCl_2 \cdot 6H_2O$, and 1.8 mM $CaCl_2$. The aorta was quickly cannulated and retrograde perfused with the same cold, high-potassium Tyrode′s solution. The right coronary artery was sutured closed and the right ventricular free wall, both atria, and most of the septum were removed to isolate the left ventricular free wall (16). The AV node was cauterized.

The tissue was submerged in a heated bath and perfused with a 37-38°C oxygenated Tyrode′s solution identical to the above but with 4.5 mM KCl. In 10 out of 14 animals, 15 mM of the excitation-contraction uncoupler 2,3-butanedione monoxime (BDM) was added to the perfusate. A constant-flow perfusion system was used with no recirculation of perfusate. Perfusion pressure was maintained between 35-45 mmHg by adjusting the flow rate. Tissue equilibrated for 90 minutes.

Action Potential Recordings

In 10 out of 14 animals, hearts were stained with the voltage-sensitive dye di-4-ANEPPS by perfusing with 50 mL of Tyrode's solution containing 5 μM dye. Optical action potentials were recorded with up to six small-diameter optical fibers (105 μm core, NA=0.22) placed against the epicardium. Excitation light from two 5 mW green lasers (532 nm) was coupled into the fibers, and fluorescence was collected from the tissue with the same fibers. A dichroic mirror was used to separate the two wavelengths of light (excitation and fluorescence). Fluorescence was longpass filtered at 590 nm and detected with a photodiode. This optical recording system is described in more detail in previous publications (14,31). The tissue ECG was recorded with two silver-silver chloride electrodes placed in the bath with positive and negative electrodes positioned near the apex and base, respectively. All signals were displayed continuously using LabView software (National Instruments Corp., Austin, TX, USA).

Optical signals and ECG were bandpass filtered from 0.1-500 Hz, digitized at 12 bit resolution, and sampled at a rate of 1 kHz per channel. Post-processing was performed using MATLAB software (MathWorks, Inc., Natick, MA, USA). Optical action potentials were digitally filtered with a 15-point median filter. The median filter was chosen because it accurately preserves the shape and timing of both upstroke and repolarization dynamics (46).

Microelectrode Recordings

In four animals, experiments were performed without the use of BDM. Action potentials were recorded from the epicardium with 1-3 floating microelectrodes (16). Microelectrode capacitance was offset using feedback through a driven shield set to approximately 80% of the ringing threshold. Data were low pass filtered (500 Hz), digitized at 16 bit resolution, and sampled at 2 kHz. The pacing protocol and data analysis were the same as for optical recordings. Attempts were made to maintain impalement throughout the entire pacing protocol. However, for quality control, only action potentials with sharp upstrokes and amplitudes greater than 70 mV were used for analysis.

Perturbed Downsweep Pacing Protocol

The tissue was paced epicardially from a bipolar electrode with 2 ms pulses at twice the diastolic threshold. Restitution properties were studied using a modified version of the perturbed downsweep protocol (PDP) previously described by Tolkacheva et al. (41) and implemented in pieces of bullfrog myocardium by Kalb et al. (20). In the PDP used by Kalb et al. (20), a downsweep in basic cycle length (BCL) was performed, with 60 seconds of pacing at each BCL_n in the downsweep. After 60 seconds of pacing at each BCL_n, single stimuli were applied at long and short coupling intervals of $BCL_{L,S} = BCL_n \pm \delta$, with 5 stimuli at BCL_n between

the two. Twenty more stimuli were applied at BCL_n before moving to BCL_{n+1} and repeating the above sequence.

The PDP was modified for our rabbit experiments to reduce the amount of continuous time spent pacing at short cycle lengths. This was done to potentially reduce tissue hypoxia that could occur due to perfusion with a non-blood solution during a period of high metabolic demand. The PDP was divided into segments, called runs, each consisting of two decrements in BCL. Between runs the tissue was paced at a recovery cycle length, $BCL_0 = 1000$ ms, for a minimum of two minutes. A graphical outline of one run is shown in Figure 1. Beginning at BCL_0, cycle length was abruptly shortened to BCL_1, and paced for 60 s. BCL was again decremented to BCL_2, and paced for 60 s. One stimulus was applied at a long cycle length, $BCL_L = BCL_2 + \delta$, followed by 5 stimuli at BCL_2. Then one stimulus was applied at a short cycle length, $BCL_S = BCL_2 - \delta$, followed by 20 stimuli at BCL_2 before returning to BCL_0. The S2 perturbation size δ was varied from 20 to 50 ms. Action potentials were recorded continuously during each run. Each modified PDP consisted of 5-7 runs with different values of BCL_1 and BCL_2 in each run.

Experimental Design

Restitution properties were determined at three epicardial locations (apex, mid-ventricle, base). In five animals, three PDPs were performed per animal with the stimulus located at the apex during one downsweep, the middle during another, and the base during another, as shown in Figure 2A. The order of sites was changed for each animal. Action potentials were recorded at a single epicardial location within 3 mm of the stimulus. Within each PDP, the runs were not ordered with decrementing BCL, but were instead randomized. In another five animals, two PDPs were performed per animal with the stimulus located at the apex and base of the epicardium, as shown in Figure 2B. The stimulus order was changed for each animal. Action potentials were recorded simultaneously from multiple epicardial sites grouped in three locations: apex, mid-ventricle, and base. Within each PDP, the runs were performed in decrementing order. It was determined from the first 5 animals that randomization of the runs was not necessary.

Determination of Restitution Portraits

Action potential duration (APD) and diastolic interval (DI) were measured between the time of maximum upstroke velocity and 70% of repolarization. Pairs of APD and preceding DI, (DI_n, APD_{n+1}) measured during the PDP, were grouped into the three response types of the RP: the dynamic restitution curve (RC), the S1-S2 RC, and the short-term memory response.

The dynamic RC measures steady-state behavior over the range of cycle lengths that produce 1:1 (stimulus:response) rhythms. At each BCL_1 and BCL_2, the last ten (DI_n, APD_{n+1}) pairs after 60 seconds of pacing were averaged to obtain steady-state points (Figure 1). All steady-state APD_{n+1} were plotted as a function of DI_n to form the dynamic RC. The slope was determined by fitting the data to an exponential equation of the form:

$$APD_{n+1} = a - be^{-DI_n/\tau_D}. \quad (1)$$

The S1-S2 RC measures the deviation from steady-state in response to a single premature or postmature stimulus. In contrast to previous studies in which the slope was evaluated as a function of the S2 interval with the S1 interval fixed (9,11,12), we obtain the slope as a function of the S1 interval. Specifically, at each BCL_2, a small section of the S1-S2 RC was formed from the steady-state response and the responses to BCL_L and BCL_S. These three (DI_n, APD_{n+1}) responses were fit to a straight line by least-squares linear regression. The slope was determined from the fitted line. Thus, in this study the slope of the S1-S2 RC is evaluated at

the steady-state of each BCL (S1), and consequently reflects the stability of the steady-state responses to small perturbations in pacing rate.

The short-term memory response measures the transient response after a step-change in BCL from steady-state at a preceding BCL. This response is also referred to as the constant BCL response (20) or accommodation (43). Short-term memory responses were obtained from the full 60 seconds of pacing at each BCL_1 and BCL_2. The magnitude of the step-change in BCL (Δ) was divided into two groups. A large step (Δ = 500 - 850 ms) was used for the transition from BCL_0 to BCL_1, and a small step (Δ = 50 - 100 ms) was used for the transition from BCL_1 to BCL_2. At each $BCL_{1,2}$, the change in APD as a function of time was fit to an exponential of the form:

$$APD(t) = c + de^{-t/\tau}. \quad (2)$$

Determination of APD Alternans

The presence of beat-to-beat alternation in APD, or alternans, was detected using a frequency spectrum analysis method similar to a method that is commonly used to detect T-wave alternans (15,30). In contrast to T-wave alternans detection, which performs analysis on vectors of time-aligned voltage signals, this method uses vectors of APD (in units of ms) in order to detect only repolarization alternans and not conduction time alternans. Analysis was performed on overlapping epochs of 64 consecutive APDs recorded during BCL_1 and BCL_2 of each PDP. Within each epoch a power spectrum estimate was calculated from the discrete Fourier transform of the autocorrelation function of the vector of 64 APDs. The presence of alternans corresponds to a peak in the power spectrum at 0.5 cycles/beat. The total alternans power is found by subtracting the mean noise in an adjacent spectral band from the alternans peak. The alternans magnitude is equal to two times the square root of the total alternans power. The K-score was calculated as a statistical measure of the degree of alternation relative to the noise in an adjacent spectral band. Significant alternation was considered present if the total alternans power was greater than 3 standard deviations of the noise band and the alternans magnitude exceeded 4 ms. This detection algorithm was tested with a false signal containing noise and a detection threshold of 4 ms alternans magnitude was determined. Persistent alternans was defined as significant alternation that persisted for the entire 60 seconds of pacing at $BCL_{1,2}$. Transient alternans were defined as significant alternation in at least one but not all epochs during $BCL_{1,2}$ pacing.

Statistical Analysis

Steady-state APD, RC slopes and short-term memory time constants were compared across pacing and recording sites using a repeated measures analysis of variance (ANOVA). Slopes of dynamic and S1-S2 RCs measured prior to 1:1 (normal) and 2:2 (alternans) responses were also compared using a repeated measures ANOVA. Results with $p < 0.05$ were considered statistically significant. Values are given as least squares mean ± standard error unless otherwise stated.

Results

Restitution Portrait in Rabbit Ventricle

In 10 animals, a total of 24 perturbed downsweep protocols were performed. During each perturbed downsweep protocol, RPs were recorded from up to six epicardial sites. A total of 47 RPs were obtained. Figure 3 shows an example of one RP recorded from the mid-ventricular region of the epicardium while the tissue was paced from a nearby mid-ventricular site (see pacing protocol, Figure 2A). In this case, alternans was not induced. Distinct restitution responses were present: response to steady-state pacing (dynamic RC), response to single

premature and postmature paced beats (S1-S2 RC), and transient response following an abrupt change in cycle length (short-term memory).

The dynamic RC forms the backbone of the RP. Its fit to Equation 1 is represented by a thin solid line in Figure 3 and individual steady-state points are represented by open circles. The S1-S2 RC is dependent on the S1 pacing interval (9). Each RP contains a set of S1-S2 RCs for different S1 values corresponding to the values of BCL_2. In Figure 3, the five S1-S2 RCs are represented by solid line segments, and the responses to BCL_L and BCL_S are marked by + and ×, respectively. The slope of the S1-S2 RC assessed at the steady-state point for a given BCL was generally smaller than the slope of the dynamic RC. This is due to the dependence of APD on pacing history (short-term memory). Following a change in pacing rate, APD continues to decrease and DI to increase, thereby increasing the slope of the dynamic RC as steady-state is approached.

The short-term memory response elicited from a step-change in BCL of size Δ is represented by filled circles in Figure 3. During the short-term memory response, there is an initial relatively large change in APD and DI in the first beat (analogous to an S1-S2 response), followed by a slow monotonic decrease in APD and increase in DI to reach steady-state (see Figure 6). Because APD and DI change only gradually during this response, these points fall on a line with a slope of -1 (20), although this is not immediately obvious in Figure 3 due to the scale of the axes. In each run of the PDP, two short-term memory responses were observed due to two step changes: BCL_0 to BCL_1 (large Δ) and BCL_1 to BCL_2 (small Δ). For visual clarity, only the latter response is shown in Figure 3.

Spatial Heterogeneity of Restitution Properties

Each component of the RP was compared among pacing and recording sites to investigate whether there were spatial differences in the restitution properties in the rabbit epicardium that were repeatable among animals.

Dynamic Restitution—Steady-state APD did not depend significantly on pacing or recording site when pacing at a BCL of 1000 ms or when pacing at shorter BCLs. This means that there was no persistent APD gradient from apex to base across the rabbit epicardium, and that there was no consistent relationship between pacing site and APD, or between distance from the pacing site and APD. However, the lack of any persistent spatial dependence of APD does not mean that APD was identical at all recording sites. Of the 9 RPs where multiple simultaneous recording sites were used, 7 had statistically significant differences in steady-state APD at BCL = 1000 ms, and 4 had statistically significant steady-state differences at BCL = 200 ms. However, these APD differences varied in magnitude and direction between animals. At BCL = 1000 ms, the difference in steady-state APD between recording sites ranged from 0 to 27 ms on average.

In Figure 4A, the slopes of all dynamic RCs (n = 33, all animals) are shown as a function of BCL. The dynamic RC slope increased as BCL was decreased from 1000 to 140 ms. The mean maximum slope of the dynamic RC was 0.78 ± 0.11 (n = 33, all animals), and only 7 of 33 dynamic RCs had a maximum slope greater than 1. Summary data for the maximum dynamic RC slope and steady-state APD are given in Table 1 as a function of recording and pacing sites. At all BCLs tested, no significant differences in dynamic RC slope were found with respect to pacing site (see Figure 5A) or recording site. Maximum dynamic RC slope also did not depend significantly on pacing site or recording site.

S1-S2 Restitution—In Figure 3, five segments of S1-S2 RC are shown. In this example, two of the five S1-S2 RCs had a negative slope. Over all S1 cycle lengths tested in all animals, 30% of the S1-S2 RCs had negative slope. In Figure 4B, the slopes of all S1-S2 RCs are shown

as a function of BCL. S1-S2 RC slope depended significantly on stimulus site: the slope was steeper when pacing from the apex than when pacing from the base ($p = 0.015$). Comparison was not possible with the mid-ventricle because tissue was not paced from this location in the experimental design of Figure 2B. Figure 5B shows the slope of the S1-S2 RC as a function of BCL when pacing from the apex and the base. The largest difference in slope occurs at BCLs less than 300 ms. S1-S2 slope did not depend significantly on recording site. The mean maximum S1-S2 slope over all animals was 0.13 ± 0.02, and the maximum slope never exceeded 1. Maximum S1-S2 RC slope did not depend significantly on pacing or recording site. Summary data for the maximum S1-S2 RC slope is given in Table 1 as a function of recording and pacing sites.

In the first beat after a sustained step-change in BCL, APD did not always decrease as expected. In both Figures 6A and 6B, when BCL was abruptly decreased APD initially increased. In Figure 3, the responses to small step-changes in BCL also showed an initial increase in APD, such that the first APD of each short-term memory transient is longer than the previous steady-state APD. A prolonged initial APD was observed in 69.3% of the short-term memory responses to a large Δ, and in 16.3% of the responses to a small Δ. This is consistent with the finding of negative S1-S2 RC slopes, although a quantitative comparison is not possible because the step-changes in BCL for S1-S2 and short-term memory responses were not of equal size.

Short-Term Memory Response—Figures 6A and 6B show examples of short-term memory responses recorded from the apex, mid-ventricle, and base from two different animals in response to large step-changes in BCL. In Figure 6A, the three responses were not measured simultaneously, but were instead measured within a few millimeters of the pacing site, and the stimulus was moved for each recording (see Figure 2A). In Figure 6B, all three recordings were made simultaneously while the tissue was paced from the base (see Figure 2B). There were significant spatial differences in the short-term memory response following a large step-change in BCL. The mean time constant of the decay, τ, is plotted in Figure 7 as a function of recording site. In Figure 7A, the data are shown for pacing and recording from the same region. The time constant was significantly shorter in the mid-ventricular region than in the apex (19.1 ± 1.1 s vs 26.5 ± 1.3 s, $p < 0.01$) or base (19.1 ± 1.1 s vs 23.5 ± 1.2 s, $p = 0.03$). In Figure 7B, the data are shown for recording at different distances from the pacing site. In this case, there were no significant differences in τ among recording sites. Interestingly, for the mid-ventricle, τ was significantly shorter when pacing in the same region compared to pacing from the apex or base (19.6 ± 4.5 s vs 38.6 ± 3.5 s, $p = 0.02$). There were no significant differences in τ between the two experimental designs when recording in the apex or base regions. In the case of small step-changes in BCL, there were no significant spatial differences in τ with respect to recording or pacing site.

The time constants of all short-term memory responses from all animals are shown in Figure 8. The time constant was determined in units of time (τ (s)) and is plotted as a function of BCL for large and small BCL step-sizes (Figures 8A and 8B, respectively). In addition, τ was determined in units of number of stimuli (τ (#beats)) and is plotted for large and small BCL step-sizes (Figures 8C and 8D, respectively). While there was a large standard deviation in τ at any given BCL, the mean τ (s) was approximately constant across BCL for both large and small step-changes in BCL. With linear regression, the mean τ (s) following large BCL steps increased by only 2.6 s for every 100 ms decrease in BCL (slope = -0.026 ± 0.009 s/ms, $p = 0.003$ vs zero). For small BCL step-sizes, the change in τ (s) as a function of BCL was statistically insignificant (slope = -0.012 ± 0.007, p = N.S. vs zero). In contrast, τ (#beats) clearly increased with decreasing BCL for both large (slope = -0.39 ± 0.04 beat/ms, $p < 0.001$ vs zero) and small (slope = -0.32 ± 0.03 beat/ms, $p < 0.001$ vs zero) BCL step-changes. The time constant was also dependent on the size of the step-change in BCL: τ was significantly

longer ($p < 0.001$) following a large Δ ($\tau = 27.1 \pm 0.9$ s) than following a small Δ ($\tau = 20.2 \pm 0.9$ s).

Incidence of APD Alternans

Alternans was observed in 7 of 10 animals and during 12 of 24 PDPs. A total of 18 RPs were measured that contained alternans. Figure 9 shows examples of action potentials recorded during a normal 1:1 response, alternans, and a more complex response, and Table 2 lists the corresponding slopes of the dynamic and S1-S2 RCs. The slopes are given at BCLs immediately preceding the shortest BCL eliciting a 1:1 response, and are compared with slopes immediately preceding 2:2 (alternans), and complex (all responses other than 1:1 and 2:2) responses. The slope of the dynamic RC was not significantly different preceding alternans than 1:1 responses (Table 2, p = N.S.), but it was significantly steeper preceding complex responses than 1:1 responses ($p < 0.01$). The slope of the S1-S2 RC was steeper preceding alternans than 1:1 responses ($p < 0.01$), and also steeper preceding complex responses than 1:1 responses ($p = 0.01$). When recording at multiple epicardial sites (as in Figure 2B), transient alternans and 1:1 responses often coexisted. At the longest BCL eliciting transient alternans, alternans always occurred at a measurement site that was farthest from the stimulus. When pacing from the apex, alternans first occurred at the base (n=3), and when pacing from the base, alternans first occurred at the apex (n=3). Alternans never occurred first at the mid-ventricle. In each case, alternans only occurred closer to the stimulus when pacing at shorter BCLs. In 8 of 18 RPs with alternans, a “bubble” of persistent alternans was seen, where stable 1:1 responses were observed at both longer and shorter BCL than the range of BCL with 2:2 responses.

Comparison with Microelectrode Recordings

The potential impact of BDM on the RP was tested in preparations (n=4) in which no BDM was used and action potentials were recorded with microelectrodes. Mean steady-state APD at $BCL_0 = 1000$ ms was 168.7 ± 5.1 ms, compared with 110.6 ± 2.9 ms in the experiments with BDM (see Table 1). At BCL = 200 ms, mean steady-state APD was 82.0 ± 3.0 ms, compared with 91.0 ± 3.2 ms for the experiments with BDM. The mean maximum dynamic RC slope was 0.95 ± 0.09, which was larger than the maximum slope with BDM (0.78 ± 0.11, Table 1). The mean maximum S1-S2 RC slope was 0.13 ± 0.03, which is indistinguishable from the maximum slope with BDM (0.13 ± 0.02, Table 1). The slope of the S1-S2 RC was larger when pacing at the apex (0.032 ± 0.012) than at the base (0.027 ± 0.011), and still larger when pacing at the mid-ventricle (0.090 ± 0.012). While sample sizes were not large enough to determine if these differences were statistically significant, the spatial trend in the data parallels the results with BDM.

The mean time constant of the short-term memory transient was larger following large step-changes in BCL ($\tau = 38.2 \pm 3.3$ s) than following small steps ($\tau = 27.8 \pm 2.8$ s), which was also the case for the data measured with BDM. When recording close to the stimulus (experimental design of Figure 2A), the time constants following large steps were 38.6 ± 7.1 s, 37.2 ± 7.8 s, and 39.0 ± 6.6 s for sites at the apex, mid-myocardium, and base, respectively. The time constant was shortest at the mid-myocardium, as was also seen in Figure 7A for the data with BDM. When recording at a distance from the stimulus (experimental design of Figure 2B), the time constants following large steps were 36.4 ± 6.1 s, 37.7 ± 5.1 s, and 40.4 ± 5.7 s for recording at the apex, mid-myocardium, and base. The trend is not exactly the same as the comparable data measured with BDM (Figure 7B), but no significant spatial differences in time constants were present in the BDM data. Time constants measured in units of time (s) did not change significantly as a function of BCL. This is consistent with the data measured with BDM, in which the time constants were more dependent on BCL when measured in number of beats than when measured in units of time (Figure 8).

Discussion

Restitution Portrait in Mammalian Tissue

This study has measured, for the first time, the restitution portrait in mammalian tissue. The RP in rabbit ventricular tissue had many similar features to those previously reported in frog ventricular tissue (20) and rabbit and guinea pig isolated myocytes (40). Each contained distinct restitution responses for the dynamic RC, S1-S2 RC, and short-term memory response. Quantitatively, both the frog and mammalian cells exhibited a larger dynamic range of APD and a steeper dynamic RC than did rabbit ventricle, but the slope of the S1-S2 RC was similar in all three studies (20,40).

The S1-S2 RC exhibited both positive and negative slope values. A negative S1-S2 RC slope resulted when a premature S2 stimulus elicited an APD that was longer than the steady-state APD at the S1 interval. A similar behavior was seen in the initial response to a sustained change in pacing rate (also an S1-S2 response). This response type has been termed supernormal (6) and appears to be a prevalent response in rabbit epicardium. It can be elicited by both a small change in BCL (as in the S1-S2 RCs) and a large change in BCL, but was more prevalent in response to a large change in BCL: APD initially increased in over half of the responses to large decrements in BCL. This response type is similar to biphasic S1-S2 RCs measured in the right ventricles of humans (11). In those patients, a full S1-S2 RC was measured for a fixed S1 value. These RCs had a local maximum around a DI of 50 ms, and had negative slope for a range of DI larger than 50 ms. A response of this type has also been observed in other species including dog (17), cat (5), and sheep (26).

Short-Term Memory—In the rabbit ventricle, the short-term memory transient followed an exponentially decaying time course with a mean time constant of 27.1 ± 0.9 seconds. Many other species have similar exponentially decaying transients. In humans, Franz et al. (11) reported the time to reach steady-state after an abrupt change in pacing rate was 2.6 ± 0.5 minutes. Time constants reported in guinea pig (45), canine (36), and frog (20) ranged from 20 - 70 seconds. In rabbit isolated myocytes, the time constant ranged from approximately 30 - 50 seconds (40). These values are all remarkably similar considering the differences in species and preparations. Short-term memory has been attributed to slow changes in intracellular or extracellular ionic concentrations, but the exact mechanism is not clear. Miyata et al. (24) note that the time course of changes in extracellular potassium concentration after a change in pacing rate closely matches the time course of changes in APD. Williams et al. (45) presented evidence that the short-term memory time constant may be linked to the inward rectifier potassium current (I_{K1}) and hypothesized that inter-species similarities are due to the ubiquitous nature of I_{K1}.

We observed that the time constant of short-term memory (τ (s)) was independent of pacing rate. The time to reach steady-state APD did not depend on a specific number of action potentials, but rather on a specific length of time, regardless of pacing rate. In rabbit and guinea pig single cells, τ decreased linearly with decreasing BCL (40). The reason that τ is dependent on BCL in rabbit single cells and is independent of BCL in coupled rabbit tissue is not clear from these two studies. It may be related to handling of extracellular potassium in restricted (coupled tissue) versus non-restricted (isolated cell) extracellular space. In our study, the time constant of short-term memory was dependent on the size of the step-change in BCL; more time was needed to recover from a larger step-change. This implies that the time constant may be related to the difference in steady-state APD at the two pacing rates.

Spatial Differences in Restitution Properties

Dynamic RC & S1-S2 RC—Spatial heterogeneity of restitution can be of two types: it can form spatial patterns that are repeatable from animal to animal, or it can have no consistent spatial patterns. We do not focus in great length on the latter because our limited number of recording sites prevents adequate measurement of epicardial dispersion of APD.

In this study, 78% of the RPs had significant spatial differences in steady-state APD at BCL = 1000 ms, whereas 44% did at BCL = 200 ms. These data suggest that spatial differences in APD exist at steady-state. However, these spatial differences did not form repeatable patterns. This study found no significant consistent spatial gradients of steady-state APD with respect to either pacing or recording site at either long or short BCL. Previous studies have found conflicting results on epicardial gradients of steady-state APD in the rabbit. Some have reported longer APDs at the apex than the base (18), while others have reported longer APDs at the base than the apex (23), and yet others have found no difference (48). We conclude that while some amount of heterogeneity may exist, there is little evidence in this study for a consistent pattern of differences in steady-state APD across the rabbit epicardium.

The dynamic RC and the S1-S2 RC did not have consistent spatial differences across the rabbit epicardium with respect to the recording site. Neither dynamic nor S1-S2 restitution curves, the most commonly used measures of restitution, were found to differ substantially in the three epicardial recording regions tested: apex, mid-ventricle, and base. We conclude that the classical restitution measures (steady-state APD, slopes of dynamic and S1-S2 RCs) show little spatial dependence in the rabbit epicardium under normal conditions.

However, the slope of the S1-S2 RC was dependent on the pacing site. The slope was steeper when pacing from the apex than from the base. APD restitution is affected by both pacing location and direction of propagation (39). Electrotonic interactions are affected by stimulation because the stimulus current produces an electrotonic load imbalance near the stimulus site, which can prolong APD in the region local to the stimulus (22,39). However, Sampson et al (39) showed that adding transmural heterogeneity into a simulated rabbit ventricle reduced steady-state APD prolongation near the stimulus, compared with a homogeneous rabbit ventricle. This is in agreement with our finding that steady-state APD and dynamic RC slope did not differ significantly at the pacing site. The effect during non-steady-state pacing is not known. It is possible that electrotonic effects at the site of stimulation may impact transient responses (S1-S2, short-term memory) more than the steady-state response.

In addition, direction of propagation relative to fiber direction in anisotropic tissue has been shown to affect electrotonic interactions, conduction velocity, and APD (47). Previous studies have shown that APD is longer during longitudinal versus transverse propagation (13,28). Fiber direction in the rabbit left ventricle varies significantly across the epicardium and fiber direction is likely different in each of the three regions of interest in this study, apex, mid-ventricle, and base (42). In the base and mid regions of the recording area the fiber direction runs predominantly along the long axis of the left ventricle, but the apical fiber direction is predominantly perpendicular to the long axis (42). The difference found in S1-S2 RC slope when pacing site was moved implies that tissue heterogeneities exist, whether structural or functional, and the S1-S2 restitution response is affected differentially by the change in stimulus location and the change in the direction of propagation.

Short-Term Memory—The time to reach steady-state APD after an abrupt shortening of cycle length was found to have repeatable spatial heterogeneity in the rabbit epicardium. We found that the time constant of the short-term memory transient near the pacing site depended on epicardial location: it was significantly shorter in the mid-ventricle than at the apex or base. However, the time constant measured farther from the pacing site was spatially uniform and

did not depend on pacing site. The differences in time constant measured close to the stimulus may result from local differences in wavefront propagation relative to fiber direction or from electrotonic effects near the site of stimulation, as discussed in the previous section. The differences may also be related to spatial heterogeneity of specific ion channel densities such as the apex to base gradients in the delayed rectifier K^+ currents, I_{Kr} and I_{Ks} (7). Whether the heterogeneity is structural or functional in nature, its existence becomes apparent when the local electrical load is modified by the pacing stimulus.

Rosenbaum et al (38) measured the first 25 beats after a change in cycle length from 500 to 300 ms in guinea pig, and found that epicardial dispersion of repolarization decreased in the first 10 beats at the new cycle length, and then increased. This transient change in dispersion may be due to spatial heterogeneity of the short term memory time constant, although such heterogeneity has not been shown in guinea pig.

Alternans—We found that the dynamic RC slope was significantly less than unity immediately preceding alternans. In addition to having slope less than unity, the dynamic RC was also not significantly steeper preceding alternans than preceding 1:1 responses. Even though the S1-S2 RC remained shallower than the dynamic RC, and always less than unity, its slope was positively correlated with the onset of alternans. These findings confirm previous research that reported alternans in the presence of RC slope less than one (12,35), in disagreement with the restitution criterion proposed by Nolasco and Dahlen (27). However, this restitution criterion is based on a one-dimensional concept of restitution, in which APD is strictly a function of the preceding diastolic interval. This relationship does not hold for tissue with memory, as evidenced by distinct dynamic, S1-S2, and constant BCL responses (8,9,20, 43). For tissue with memory, the alternans criteria take the form of a combination of slopes: the combination can be equal to one, while individual slopes can be quite different than one (41). Others have suggested that APD restitution alone may not determine the onset of alternans; factors such as spatial heterogeneity of restitution (25), conduction velocity restitution (8,10), or calcium cycling (12,32) may also play a role.

Alternans was observed to form at the recording site most distant from the stimulus at a slower pacing rate, and was seen in more proximal locations only after the rate had been increased. Both experiments and models have found this same behavior (8,10). This phenomenon may be due to spatial gradients of restitution properties that are induced by pacing and boundary effects, although significant gradients distal to the stimulus were not observed.

Impact of BDM on Restitution Responses

In previous studies the electromechanical uncoupler BDM was shown to have the following effects on restitution: it decreases steady-state APD (4,35), decreases the maximum slope of the dynamic restitution curve (4,35), and can either decrease the amplitude of alternans (35) or decrease the occurrence of alternans (4). While most of the experiments presented here were performed with BDM, a small subset (n=4) of the studies were performed in the absence of BDM. Qualitatively, the RPs with and without BDM were very similar. In both cases, the S1-S2 RCs were more shallow than the dynamic RC at all BCL. The short-term memory transients followed exponentially decaying time courses with similar time constants in both sets of experiments. Some quantitative differences were found in the restitution responses. First, at BCL = 1000 ms, steady-state APD was longer in preparations without BDM compared to those with BDM (168.7 ± 5.1 ms versus 110.6 ± 2.9 ms). APD differences were much smaller between the two groups at short BCLs. Second, the mean maximum dynamic RC slope was larger without BDM (0.95 ± 0.09) compared to with BDM (0.78 ± 0.11). Third, the time constants of the short-term memory transients were longer in experiments without the use of BDM (38.2 ± 3.3 s, large BCL step-change) than those with BDM (27.1 ± 0.9 s, large step-

changes). The changes seen in steady-state APD and dynamic RC slope confirm previous research (4,35).

Other restitution properties remained unchanged. The mean maximum slope of the S1-S2 RC was unaffected by the use of BDM. Also, the behavior of the short-term memory time constant was consistent in both sets of experiments: the time constant was shorter following a smaller step-change in BCL, and it was independent of the value of the BCL. We also investigated the spatial differences in restitution properties and found similar trends with and without BDM. Specifically, the S1-S2 RC was steeper when pacing from the apex than from the base. Also, when pacing and recording in the same epicardial region, the time constant was shorter at the mid-ventricle than at the apex or base.

Implications and Limitations

Two characteristics of the restitution portrait were found to have repeatable spatial heterogeneity with respect to the pacing site: the time constant of the short-term memory transient in response to local stimulation and the S1-S2 RC slope. The presence of these two transient spatial heterogeneities following a change in pacing rate may affect electrical stability at the onset of a tachycardia or during a series of rapid ectopic beats, both common precursors to ventricular fibrillation. Our results predict that the restitution response of tissue to tachycardia or ectopy may be different than the response to similarly timed sinus beats. Vulnerability may be affected by the location of origin of the abnormal beats. The mechanism for this would be two-fold: the restitution properties near the site of origin of the beats may change depending on location, and the spatial dispersion of repolarization farther from the site of origin may also be altered, creating a period of higher vulnerability during the first few beats of ectopy or tachycardia.

The finding of these repeatable spatial heterogeneities of restitution (S1-S2 and short-term memory) also has implications for future research. With classical restitution measures (the dynamic and S1-S2 RCs), the transient heterogeneity of short-term memory would not have been discovered. This study illustrates the need for more complete characterization of the multiple aspects of restitution. The perturbed downsweep protocol and the restitution portrait are useful techniques for this purpose.

This study was limited by the fact that action potential recordings were only obtained from a maximum of six locations at a time. This type of experimental design can be useful in detecting gradients in restitution properties across different regions of tissue (16,18,19). However, detecting the dispersion of restitution properties within a smaller area of tissue, such as has been performed previously (21,25), requires higher resolution and is therefore not possible with so few recording points. We must make the assumption that the differences within an epicardial region (apex, mid-ventricle, or base) were of smaller magnitude than the gradients in restitution properties that might exist across regions. Comparisons of restitution properties measured with and without BDM were limited by the fact that the comparisons were not made in the same animals and also by the small number of animals (n=4) in which BDM was not present. This study was also limited by the fact that APD was only recorded from the epicardium. Previous studies have shown that transmural gradients in steady-state APD exist at slow to moderate pacing rates (2,16). Thus, future work will involve transmural measurements of the restitution portrait, which would allow us to elucidate spatial differences in both steady-state and transient restitution responses.

Acknowledgements

The authors thank Daniel J. Gauthier for insightful comments and Adrian J. Lam for assistance constructing optical mapping system.

Grants: This work was supported by National Institutes of Health Grant R01-HL-72831 and National Institute of Child Health and Human Development Grant K12-HD-43494.

References

1. Akar FG, Laurita KR, Rosenbaum DS. Cellular basis for dispersion of repolarization underlying reentrant arrhythmias. J Electrocardiol 2000;33:23–31. [PubMed: 11265727]
2. Antzelevitch C, Sicouri S, Litovsky SH, Lukas A, Krishnan SC, Didiego JM, Gintant GA, Liu DW. Heterogeneity within the Ventricular Wall - Electrophysiology and Pharmacology of Epicardial, Endocardial, and M-Cells. Circ Res 1991;69:1427–1449. [PubMed: 1659499]
3. Arce H, Xu AX, Gonzalez H, Guevara MR. Alternans and higher-order rhythms in an ionic model of a sheet of ischemic ventricular muscle. Chaos 2000;10:411–426. [PubMed: 12779397]
4. Banville I, Gray RA. Effect of action potential duration and conduction velocity restitution and their spatial dispersion on alternans and the stability of arrhythmias. J Cardiovasc Electrophysiol 2002;13:1141–1149. [PubMed: 12475106]
5. Bass BG. Restitution of the action potential in cat papillary muscle. Am J Physiol 1975;228:1717–1724. [PubMed: 1155603]
6. Boyett MR, Jewell BR. Analysis of the Effects of Changes in Rate and Rhythm Upon Electrical-Activity in the Heart. Prog Biophys Mol Biol 1980;36:1–52. [PubMed: 7001542]
7. Cheng JH, Kamiya K, Liu WR, Tsuji Y, Toyama J, Kodama I. Heterogeneous distribution of the two components of delayed rectifier K+ current: a potential mechanism of the proarrhythmic effects of methanesulfonanilide class III agents. Cardiovasc Res 1999;43:135–147. [PubMed: 10536698]
8. Cherry EM, Fenton FH. Suppression of alternans and conduction blocks despite steep APD restitution: electrotonic, memory, and conduction velocity restitution effects. Am J Physiol Heart Circ Physiol 2004;286:H2332–H2341. [PubMed: 14751863]
9. Elharrar V, Surawicz B. Cycle Length Effect on Restitution of Action-Potential Duration in Dog Cardiac Fibers. Am J Physiol 1983;244:H782–H792. [PubMed: 6859281]
10. Fox JJ, Riccio ML, Hua F, Bodenschatz E, Gilmour RF. Spatiotemporal transition to conduction block in canine ventricle. Circ Res 2002;90:289–296. [PubMed: 11861417]
11. Franz MR, Swerdlow CD, Liem LB, Schaefer J. Cycle Length Dependence of Human Action-Potential Duration Invivo - Effects of Single Extrastimuli, Sudden Sustained Rate Acceleration and Deceleration, and Different Steady-State Frequencies. J Clin Invest 1988;82:972–979. [PubMed: 3417875]
12. Goldhaber JI, Xie LH, Duong T, Motter C, Khuu K, Weiss JN. Action potential duration restitution and alternans in rabbit ventricular myocytes - The key role of intracellular calcium cycling. Circ Res 2005;96:459–466. [PubMed: 15662034]
13. Gotoh M, Uchida T, Mandel WJ, Fishbein MC, Chen PS, Karagueuzian HS. Cellular graded responses and ventricular vulnerability to reentry by a premature stimulus in isolated canine ventricle. Circulation 1997;95:2141–2154. [PubMed: 9133525]
14. Idriss SF, Pitruzzello AM. A low-cost high-efficiency fiber-optic coupler for recording action potentials within the myocardial wall. Ieee Trans Biomed Eng 2006;53:1708–1711. [PubMed: 16916108]
15. Idriss SF, Van Hare GF, Fink D, Rosenbaum DS. Microvolt T wave alternans inducibility in normal newborn puppies: Effects of development. J Cardiovasc Electrophysiol 2002;13:593–598. [PubMed: 12108504]
16. Idriss SF, Wolf PD. Transmural action potential repolarization heterogeneity develops postnatally in the rabbit. J Cardiovasc Electrophysiol 2004;15:795–801. [PubMed: 15250865]
17. Iinuma H, Kato K. Supernormal Responses to Premature Stimulation in Ca-Dependent Action Potentials. Experientia 1979;35:885–886. [PubMed: 477841]
18. Iwata H, Kodama I, Suzuki R, Kamiya K, Toyama J. Effects of long-term oral administration of amiodarone on the ventricular repolarization of rabbit hearts. Jpn Circ J 1996;60:662–672. [PubMed: 8902584]
19. Janse MJ, Sosunov EA, Coronel R, Opthof T, Anyukhovsky EP, de Bakker JMT, Plotnikov AN, Shlapakova IN, Danilo P, Tijssen JGP, Rosen MR. Repolarization gradients in the canine left

ventricle before and after induction of short-term cardiac memory. Circulation 2005;112:1711–1718. [PubMed: 16157774]

20. Kalb SS, Dobrovolny HM, Tolkacheva EG, Idriss SF, Krassowska W, Gauthier DJ. The restitution portrait: A new method for investigating rate-dependent restitution. J Cardiovasc Electrophysiol 2004;15:698–709. [PubMed: 15175067]
21. Laurita KR, Girouard SD, Rosenbaum DS. Modulation of ventricular repolarization by a premature stimulus - Role of epicardial dispersion of repolarization kinetics demonstrated by optical mapping of the intact guinea pig heart. Circ Res 1996;79:493–503. [PubMed: 8781482]
22. Laurita KR, Girouard SD, Rudy Y, Rosenbaum DS. Role of passive electrical properties during action potential restitution in intact heart. Am J Physiol Heart Circ Physiol 1997;42:H1205–H1214.
23. Liu T, Choi BR, Drici MD, Salama G. Sex modulates the arrhythmogenic substrate in prepubertal rabbit hearts with long QT 2. J Cardiovasc Electrophysiol 2005;16:516–524. [PubMed: 15877623]
24. Miyata A, Dowell JD, Zipes DP, Rubart M. Rate-dependent [K+](o) accumulation in canine right atria in vivo: electrophysiological consequences. Am J Physiol Heart Circ Physiol 2002;283:H506–H517. [PubMed: 12124195]
25. Nash MP, Bradley CP, Sutton PM, Clayton RH, Kallis P, Hayward MP, Paterson DJ, Taggart P. Whole heart action potential duration restitution properties in cardiac patients: a combined clinical and modelling study. Experimental Physiology 2006;91:339–354. [PubMed: 16452121]
26. Noble D, Cohen I. Interpretation of T-Wave of Electrocardiogram. Cardiovasc Res 1978;12:13–27. [PubMed: 76514]
27. Nolasco J, Dahlen R. A graphic method for the study of alternation in cardiac action potentials. J Appl Physiol 1968;25:191–196. [PubMed: 5666097]
28. Osaka T, Tsuboi N, Kodama I, Toyama J, Yamada K. Effects of Activation Sequences and Anisotropic Cellular Geometry on the Repolarization Phase of Action-Potentials of Dog Ventricular Muscles. Jpn Circ J 1987;51:963–964.
29. Pak HN, Hong SJ, Hwang GS, Lee HS, Park SW, Ahn JC, Ro YM, Kim YH. Spatial dispersion of action potential duration restitution kinetics is associated with induction of ventricular tachycardia/fibrillation in humans. J Cardiovasc Electrophysiol 2004;15:1357–1363. [PubMed: 15610278]
30. Pastore JM, Girouard SD, Laurita KR, Akar FG, Rosenbaum DS. Mechanism linking T-wave alternans to the genesis of cardiac fibrillation. Circulation 1999;99:1385–1394. [PubMed: 10077525]
31. Pitruzzello, AM.; Krassowska, W.; Lam, AJ.; Idriss, SF. In: Hozman, J.; Kneppo, P., editors. A multichannel fiber-optic mapping system for intramural recording of cardiac action potentials; 3rd European Medical & Biological Engineering Conference; Prague, Czech Republic. IFMBE Proceedings. 2005;
32. Pruvot EJ, Katra RP, Rosenbaum DS, Laurita KR. Role of Calcium Cycling Versus Restitution in the Mechanism of Repolarization Alternans. Circ Res 2004;94:1083–1090. [PubMed: 15016735]
33. Qian YW, Sung RJ, Lin SF, Province R, Clusin WT. Spatial heterogeneity of action potential alternans during global ischemia in the rabbit heart. Am J Physiol Heart Circ Physiol 2003;285:H2722–H2733. [PubMed: 12907420]
34. Qu Z, Garfinkel A, Chen P-S, Weiss JN. Mechanisms of Discordant Alternans and Induction of Reentry in Simulated Cardiac Tissue. Circulation 2000;102:1664–1670. [PubMed: 11015345]
35. Riccio ML, Koller ML, Gilmour RF. Electrical restitution and spatiotemporal organization during ventricular fibrillation. Circ Res 1999;84:955–963. [PubMed: 10222343]
36. Robinson RB, Boyden PA, Hoffman BF, Hewett KW. Electrical Restitution Process in Dispersed Canine Cardiac Purkinje and Ventricular Cells. Am J Physiol 1987;253:H1018–H1025. [PubMed: 3688246]
37. Rosen MR. What is cardiac memory? J Cardiovasc Electrophysiol 2000;11:1289–1293. [PubMed: 11083252]
38. Rosenbaum DS, Kaplan DT, Kanai A, Jackson L, Garan H, Cohen RJ, Salama G. Repolarization Inhomogeneities in Ventricular Myocardium Change Dynamically with Abrupt Cycle Length Shortening. Circulation 1991;84:1333–1345. [PubMed: 1884456]
39. Sampson KJ, Henriquez CS. Electrotonic influences on action potential duration dispersion in small hearts: a simulation study. Am J Physiol Heart Circ Physiol 2005;289:H350–H360. [PubMed: 15734889]

40. Tolkacheva EG, Anumonwo JMB, Jalife J. Action potential duration restitution portraits of mammalian ventricular myocytes: Role of calcium current. Biophys J 2006;91:2735–2745. [PubMed: 16844743]

41. Tolkacheva EG, Schaeffer DG, Gauthier DJ, Krassowska W. Condition for alternans and stability of the 1: 1 response pattern in a “memory” model of paced cardiac dynamics. Phys Rev E 2003:67.

42. Vetter FJ, McCulloch AD. Three-dimensional analysis of regional cardiac function: a model of rabbit ventricular anatomy. Prog Biophys Mol Biol 1998;69:157–183. [PubMed: 9785937]

43. Watanabe MA, Koller ML. Mathematical analysis of dynamics of cardiac memory and accommodation: theory and experiment. Am J Physiol Heart Circ Physiol 2002;282:H1534–H1547. [PubMed: 11893591]

44. Weiss JN, Qu ZL, Chen PS, Lin SF, Karagueuzian HS, Hayashi H, Garfinkel A, Karma A. The dynamics of cardiac fibrillation. Circulation 2005;112:1232–1240. [PubMed: 16116073]

45. Williams BA, Dickenson DR, Beatch GN. Kinetics of rate-dependent shortening of action potential duration in guinea-pig ventricle; effects of I-K1 and I-Kr blockade. Br J Pharmacol 1999;126:1426–1436. [PubMed: 10217537]

46. Witkowski, FX.; Penkoske, PA.; Leon, LJ. Optimization of Temporal Filtering for Optical Transmembrane Potential Signals. In: Rosenbaum, DS.; Jalife, J., editors. Optical Mapping of Cardiac Excitation and Arrhythmias. Futura; Armonk, NY: 2001. p. 79-92.

47. Wolk R, Cobbe SM, Hicks MN, Kane KA. Functional, structural, and dynamic basis of electrical heterogeneity in healthy and diseased cardiac muscle: implications for arrhythmogenesis and anti-arrhythmic drug therapy. Pharmacol Ther 1999;84:207–231. [PubMed: 10596907]

48. Wolk R, Kane KA, Cobbe SM, Hicks MN. Apex-to-base dispersion of refractoriness underlies the proarrhythmic effect of hypokalaemia/hypomagnesaemia in the rabbit heart. J Electrocardiol 2002;35:245–252. [PubMed: 12122615]

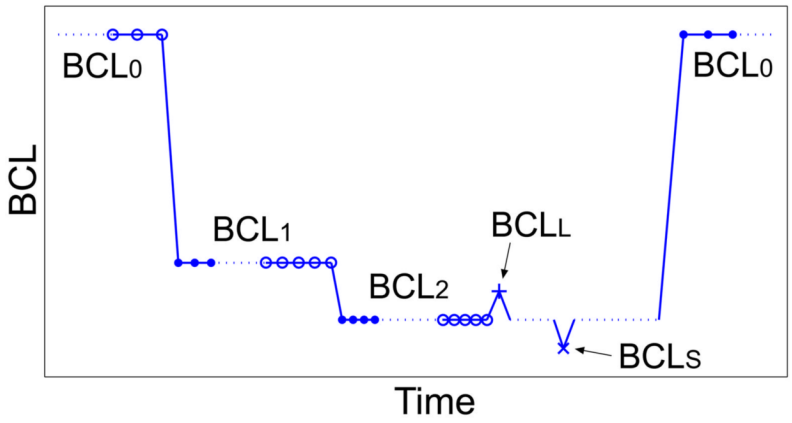

Figure 1.
Schematic of one pacing run of the modified perturbed downsweep protocol (PDP). The three different types of restitution responses shown are: dynamic RC data (○), S1-S2 RC data (+ and ×), and short-term memory responses (●).

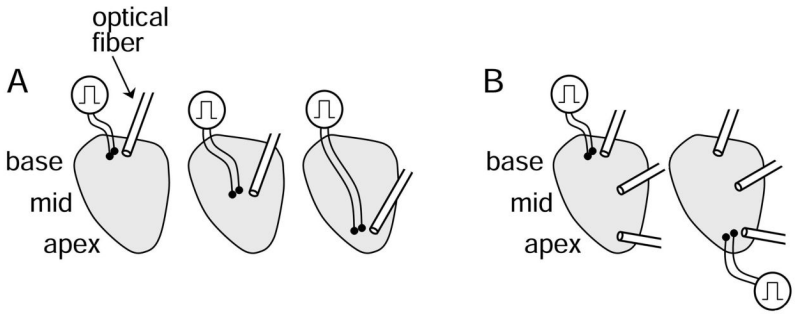

Figure 2.

Experimental design. In A, the tissue was paced from the base, mid-ventricle, and apex during separate PDPs. Action potentials were recorded optically at a single site within 3 mm of the stimulus during each PDP. In B, the tissue was paced from the base and apex during separate PDPs. During each PDP, action potentials were recorded from three regions of epicardium, the base, mid-ventricle and apex.

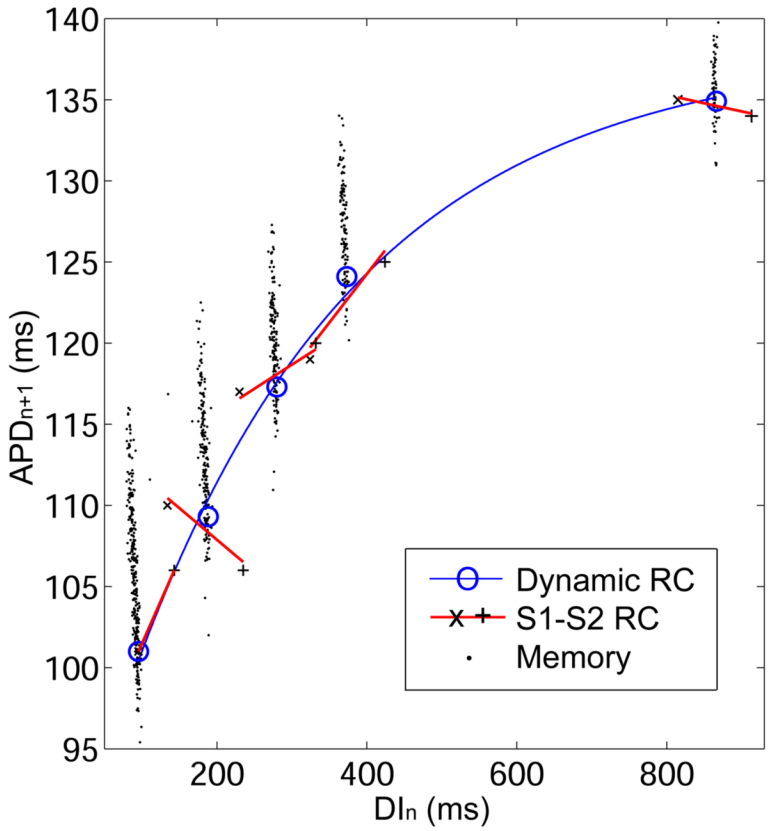

Figure 3.

Restitution portrait from one animal when pacing and recording from the mid-ventricle. The RP contains one dynamic RC (thin line) composed of steady-state points (○) from each BCL_2. At each BCL_2 there is an S1-S2 RC (thick line and ×, +), and a short-term memory response (●). At the shortest BCL_2, the S1-S2 RC has only two points because BCL_S did not elicit an action potential. At each BCL_2, all three restitution responses theoretically intersect at the steady-state point because this point is contained in each of the responses.

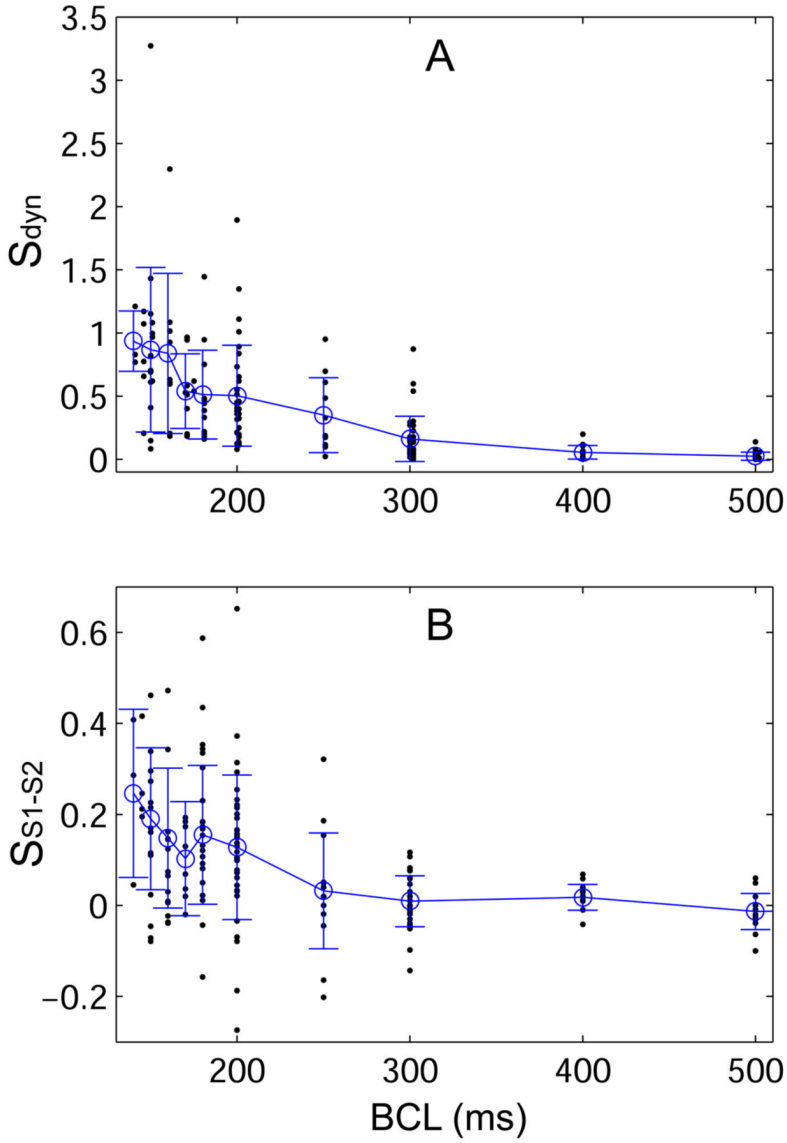

Figure 4.

Slopes of the (A) dynamic (S_{dyn}) and (B) S1-S2 (S_{S1-S2}) RCs as a function of BCL from all animals. Dots represent individual slope values, open circles indicate the overall mean slope at a given BCL, and error bars indicate the standard deviation of values at each BCL. The mean slope of the dynamic RC approaches one at the shortest BCL. The mean S1-S2 slope remains well below one at all BCL, and the maximum observed slope is less than 0.7.

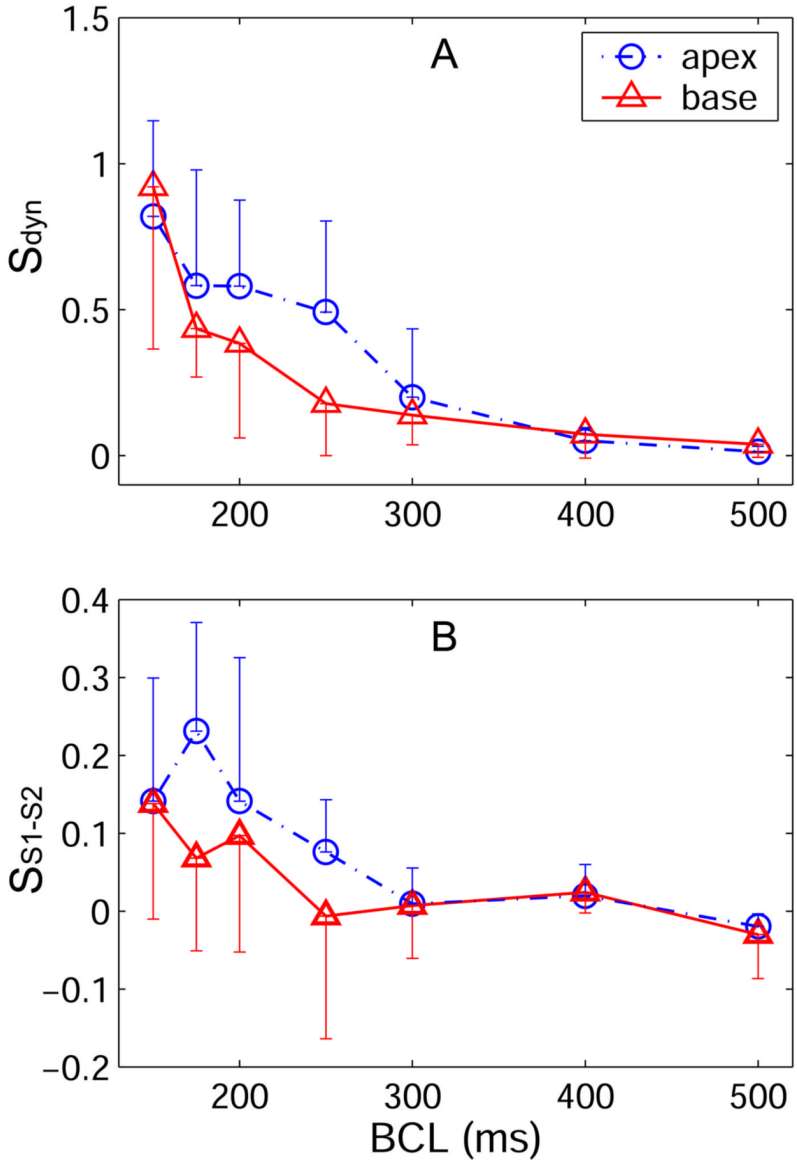

Figure 5.

Slopes of the (A) dynamic and (B) S1-S2 RCs as a function of BCL and stimulus site. Data are shown only from pacing at the apex or the base. Data recorded from all three epicardial regions is shown. For both RCs, we tested whether there was a difference in slope as a function of stimulus site using an ANOVA model that used repeated measures to account for inter-animal differences. The S1-S2 RC slope was significantly steeper when pacing from the apex compared with pacing from the base ($p = 0.015$). The difference in slope was greatest at shorter BCL. The dynamic RC slope appears steeper when pacing at the apex versus pacing at the base over the same range of BCL as the S1-S2 RC slope. Surprisingly, for the dynamic RC the difference was not found to be significant.

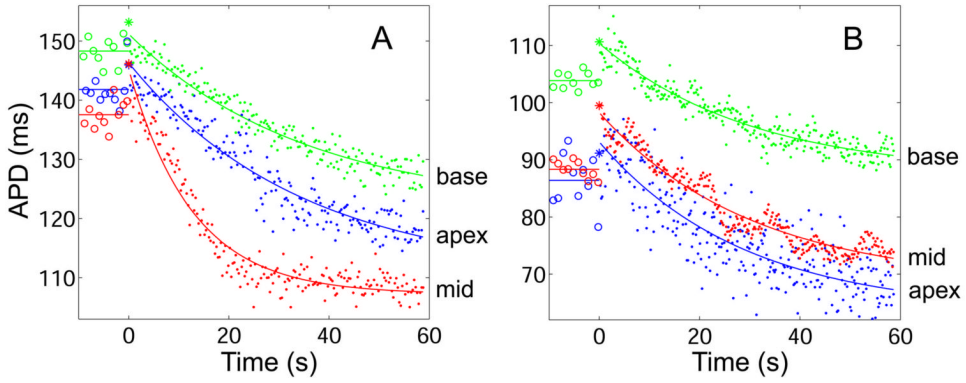

Figure 6.

Short-term memory responses recorded from the apex, mid-ventricle (mid), and base regions from two animals. At time t = 0, BCL is abruptly shortened from BCL_0 = 1000 ms to BCL_1. Shown are the last 10 steady-state APDs at BCL_0 (○, straight line at mean value), the first APD at BCL_1 (*), and all subsequent APDs at BCL_1 (●, solid line shows exponential fit). In both A and B, the step-decrease in BCL causes an initial increase in APD followed by a slow exponential decrease to steady-state. In A, the experimental design of Figure 2A was used. During three successive PDPs, responses were measured next to the stimulus while pacing and recording in the three epicardial regions. In this example, BCL_1 = 300 ms (Δ = 700 ms), and τ at the apex, middle, and base are 34.6 s, 12.7 s, and 35.1 s, respectively. In B, the experimental design of Figure 2B was used. During a single PDP, the tissue was paced from the base and the three responses shown were recorded simultaneously. In this example, BCL_1 = 200 ms (Δ = 800 ms), and τ at the apex, middle, and base are 27.3 s, 30.4 s, and 28.9 s, respectively.

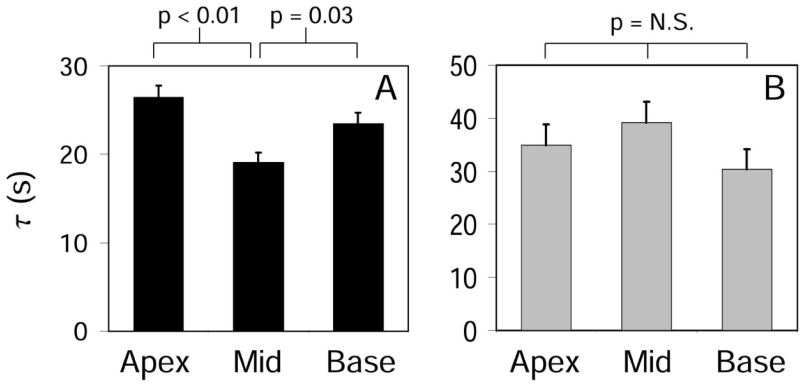

Figure 7.

Mean time constants of short-term memory in response to large step-changes in BCL. Time constants are shown by recording site. In A, the response was measured close to the pacing site using the experimental design shown in Figure 2A. Mean data from five animals is shown. The time constant was significantly shorter at the mid-ventricle ($\tau = 19.1 \pm 1.1$ s) than at the apex ($\tau = 26.5 \pm 1.3$ s) or base ($\tau = 23.5 \pm 1.2$ s). In B, the distance between recording and pacing sites ranged from a few mm to several cm, as shown in the experimental design in Figure 2B. Mean data from five animals is shown. There were no significant differences in τ among recording sites.

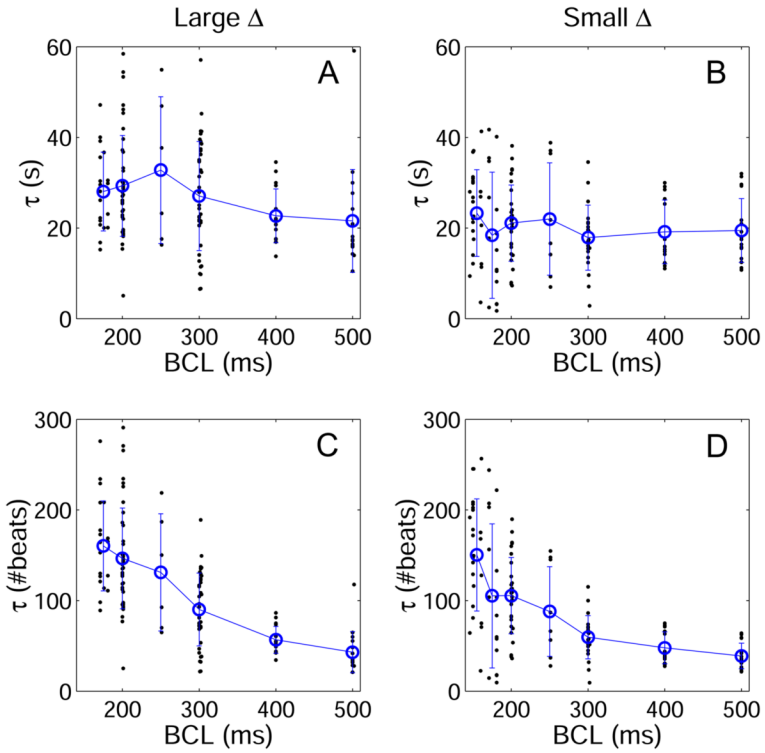

Figure 8.

Time constants (τ) of short-term memory responses resulting from both large (A,C) and small (B,D) step-changes in BCL (Δ). In A and B, τ is shown in units of time, while in C and D, τ is shown in numbers of beats. When measured in units of time, τ is approximately constant across BCL, but when measured in number of beats, τ increases with decreasing BCL. Data from all pacing and recording sites are shown together in this figure.

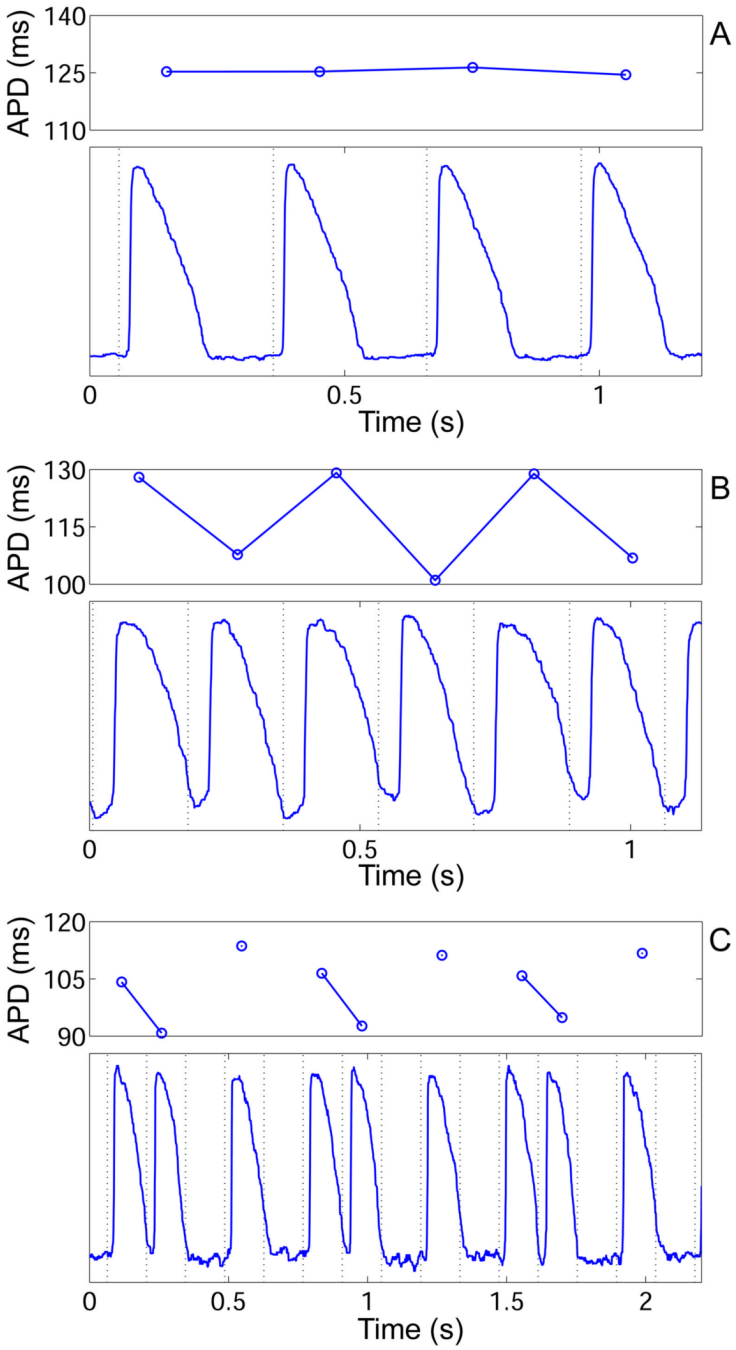

Figure 9.

APDs and the underlying action potentials recorded optically during (A) 1:1, (B) 2:2 (alternans), and (C) complex responses. Pacing and recording occurred in the base region for all panels. Dotted lines represent the pacing stimulus. In A, the BCL = 300 ms, in B, BCL = 175 ms, and in C, BCL = 140 ms. In C, the response is 3:5 (complex), so 2 out of 5 pacing stimuli do not elicit action potentials. No APD exists for these stimuli, resulting in a gap in the line connecting APDs.

Table 1

Mean Restitution Properties (n = 10) by Recording and Pacing Site

Recording Site	$S_{dyn, max}$	$S_{S1-S2, max}$	APD (ms) at BCL_0
Apex	0.73 ± 0.20	0.13 ± 0.04	103.8 ± 5.1
Mid	0.93 ± 0.21	0.15 ± 0.04	115.1 ± 5.3
Base	0.69 ± 0.19	0.13 ± 0.03	112.8 ± 4.7
Pacing Site			
Apex	0.77 ± 0.16	0.16 ± 0.03	113.8 ± 4.2
Mid	0.92 ± 0.30	0.27 ± 0.08	128.2 ± 8.4
Base	0.72 ± 0.20	0.10 ± 0.03	103.7 ± 4.0
All Sites	0.78 ± 0.11	0.13 ± 0.02	110.6 ± 2.9

Restitution properties: maximum dynamic RC slope ($S_{dyn, max}$), maximum S1-S2 RC slope ($S_{S1-S2, max}$), and steady-state APD at BCL_0 = 1000 ms. In the recording site section, data are included from all pacing sites; in the pacing site section, data are included from all recording sites. In the final section, data from all pacing and recording sites are included. Values are least square mean ± standard error.

Table 2

Mean RC slopes (n = 10) at BCLs immediately preceding 1:1, alternans, and complex responses.

Response	S_{dyn}	S_{S1-S2}
stable 1:1	0.23 ± 0.04	0.05 ± 0.01
alternans	0.39 ± 0.06	0.19 ± 0.02*
complex	0.82 ± 0.07*	0.11 ± 0.02*

Values are least square mean ± standard error.

* $p < 0.05$ vs stable1:1 response.